

Colorimetric detection of Cu^{2+} and Pb^{2+} ions using calix[4]arene functionalized gold nanoparticles

RAVI GUNUPURU^{a,b}, DEBDEEP MAITY^a, GOPALA R BHADU^a, ASHISH CHAKRABORTY^a, DIVESH N SRIVASTAVA^{a,b} and PARIMAL PAUL^{a,b,*}

^aAnalytical Discipline and Centralized Instrument Facility, CSIR-Central Salt and Marine Chemicals Research Institute, G B Marg, Bhavnagar 364 002, India

^bAcSIR-CSMCRI, G B Marg, Bhavnagar 364 002, India

e-mail: ppaul@csmcri.org

MS received 6 August 2013; revised 26 November 2013; accepted 28 November 2013

Abstract. Calixarene functionalized gold nanoparticles (CFAuNPs) have been prepared and characterized by spectroscopic and microscopic (TEM) techniques. To use this material as potential colorimetric sensor, the binding property of this new material has been investigated with a large number of metal ions. It exhibited sharp colour change from dark brown to green and blue, detectable by naked-eye, in the presence of Cu^{2+} and Pb^{2+} ions, respectively. It has also triggered substantial change in surface plasmon resonance (SPR) band of the functionalized gold nanoparticles, which in case of $\text{Pb}(\text{II})$ is due to the inter particle plasmon coupling arising from the metal-induced aggregation of the nanoparticles and for $\text{Cu}(\text{II})$, it is because of the formation of AuCu alloy due to anti-galvanic exchange. The size and aggregation of the nanoparticles are confirmed from HRTEM images, elemental analysis and the line profiling for both the metal ions have been done by STEM-EDX analysis.

Keywords. Calixarene; gold nanoparticles; colorimetric sensor; ion recognition; copper(II); lead(II).

1. Introduction

Detection of metal ions with high selectivity is an emerging area of current research because of their applications in various chemical, environmental and biological processes.^{1–5} In this context, detection of Cu^{2+} and Pb^{2+} are critically important because of their toxic impact on human health and environment.^{6–8} Although, Cu^{2+} is an essential trace element for many biological processes but its higher concentration is toxic to human body.^{9–12} Pb^{2+} is another highly toxic metal ion, a potent central neurotoxin and highly bio accumulative in bones and kidneys, resulting in damage.^{13–16} Therefore, detection of both of these metal ions is important and significant progress has been made in this direction by designing molecular sensors based on fluorescence, surface plasmon resonance, colorimetry and voltametry.^{17–21} Among these various detection techniques, colorimetric method is less studied, which in fact allow onsite naked-eye detection and do not require any specialized analytical instrument. With recent development in nanotechnology, the

metal nanoparticles are emerging as important colorimetric receptor for the designing of colorimetric sensors.^{22–30}

The gold nanoparticles are known to have one of the highest visible-region extinction coefficients ($10^9 \text{ M}^{-1} \text{ cm}^{-1}$ order) with red-wine colour due to surface plasmon resonance.³¹ This surface plasmon band is very sensitive to their particle size and to their inter-particle distance, the transition of nanoparticles from dispersion to aggregation exhibit distinct colour change because of the coupling of the plasmon absorbances and this change in optical property can be used as a tool for ion recognition event.^{32–38}

To function as probes, the nanoparticles are subjected to modification with a receptor molecule containing ionophore moiety, which can interact selectively with the analyte of interest, and a spacer that can be covalently linked to the nanoparticle surface. The covalent linking onto the surface of the nanoparticles can be achieved through Au–S or Au–N bond.^{29,31} For colorimetric sensing of metal ions, the use of functionalized gold nanoparticles have been reported recently, however in most of the cases modification of nanoparticles have been done using DNA, peptides and crown ethers.^{32–34,39–41} Calixarene functionalized gold

*For correspondence

nanoparticles are mainly used to study their properties and also as colorimetric sensors for recognition of molecules such as amino acids, pyridinium ion and quaternary ammonium ion.^{42–48}

Taking the advantage of versatile ion-recognition property of the modified calix[4]arene, gold nanoparticles were functionalized by covalent linking of a modified calix[4]arene, which provide a highly preorganized architecture for the assembling of converging binding sites. The linking of the ionophore on to the surface of the nanoparticles was performed through Au–S bond using long chain aliphatic moiety as spacer. Here, we report the synthesis of calix[4]arene functionalized gold nanoparticles and its application as a novel colorimetric sensor for Cu^{2+} and Pb^{2+} .

2. Experimental

2.1 Reagents and chemicals

Chemicals such as *tert*-butylphenol, iodopropane, 1,11-dibromoundecane, tetraoctylammonium bromide (TOAB), tetrabutyl ammonium fluoride (TBAF), hexamethyl disilathiane (Me_3Si)₂S, HAuCl_4 , NaBH_4 were purchased from Sigma-Aldrich Co. All metal perchlorate salts were purchased from Alfa Aesar (Johnson Matthey) Co. All other solvents and reagents used in this study were purchased from SD Fine Chemicals. Organic solvents used were analytical grade and were used as received for synthetic purpose. Solvents for spectral studies were freshly purified by standard procedures before use.

2.2 Instrumentation

Elemental analyses (C, H and N) were performed on a model 2400 Perkin-Elmer elemental analyzer. NMR spectra were recorded on a model DPX 200 and Avance II 500 MHz Bruker FT-NMR instruments using TMS as internal standard. Infrared spectra were recorded on a Perkin Elmer Spectrum GX FT-IR system as KBr pellets. Mass spectra were recorded on a Q-ToF microTM LC-MS instrument. The UV-Vis spectra were recorded on a CARY 500 scan Varian spectrophotometer. Transmission electron microscope (TEM) images were recorded on HR-TEM (JEOL JEM 2100). The samples were dispersed in ethanol and loaded over Lacey carbon coated Cu TEM grid (300 mesh). The samples were dried under ambient condition and imaged at 200 KV acceleration voltages. The elemental mapping of the samples was done using *in situ* EDX-STEM (Oxford instrument, INCA x-sight).

2.3 Synthesis of compounds

Calix[4]arene (**1**) and *bis*-isopropyl substituted calix[4]arene (**2**) were prepared following the literature procedures.^{49,50}

2.3a Synthesis of compound 3: This compound was synthesised following a modified published procedure used for other compound.⁴⁸ In a typical procedure, into the acetonitrile solution (20 mL) of **2** (0.5 g, 0.98 mM) 1,11-dibromoundecane (0.8 g, 2.5 mM) and K_2CO_3 (0.4 g, 2.9 mM) were added and the reaction mixture was stirred under reflux for 24 h. The solvent was then evaporated to dryness by rotary evaporation and the residue was treated with 5% HCl (20 mL), the resultant mass was extracted twice with dichloromethane (40 mL) and washed twice with water (25 mL each time). The organic phase was dried over anhydrous sodium sulphate and solvent was removed to isolate the solid mass. The crude product was then purified by column chromatography using silica gel (100–200 mesh) as packing material and 5% ethyl acetate in hexane as eluent. ¹H NMR (CDCl_3) δ 0.88–1.03 (m, 10H), 1.27–1.52 (m, 24H), 1.78–2.05 (m, 8H), 3.24 (m, 4H), 3.42 (t, 4H, $J = 7.2$ Hz), 3.83 (m, 4H), 3.96 (m, 2H), 4.08 (d, 2H, $J = 13.0$ Hz), 6.69 (t, 2H, $J = 7.0$ Hz), 6.82 (t, 2H, $J = 7.0$ Hz), 6.96 (d, 4H, $J = 7.0$ Hz), 7.05 (d, 4H, $J = 7.0$ Hz). ES-MS: m/z 1013.93 (calculated for $3 + \text{K}^+$, 1014.12); 997.92 (calculated for $3 + \text{Na}^+$, 997.97). Anal. calcd. for $\text{C}_{56}\text{H}_{78}\text{O}_4\text{Br}_2$: C, 68.89; H, 8.06; Found: C, 68.08; H, 7.94.

2.3b Synthesis of compound 4: This compound was synthesised by following a modified published procedure used for preparation of functionalized thiols of some other compounds.⁵¹ In a 50 mL RB flask, 1.0 g of **3** was dissolved in freshly distilled THF and the temperature of the solution was maintained at -5°C . To this solution, 0.6 g (2.26 mM) of tetrabutyl ammonium fluoride was added and the resulting solution was stirred for 5 min, then 440 mg (2.46 mM) of hexamethyl disilathiane was added. The reaction mixture turned initially to brown, then changed to light yellow and finally it became colourless within 30 min. The reaction mixture was then diluted by adding dichloromethane (20 mL) and stirred for 5 min. The resultant mixture was then washed twice with saturated aqueous NH_4Cl (15 mL each time) and finally with water. The organic layer was then dried over anhydrous sodium sulphate and the solvent was removed by rotary evaporation. The crude product was purified by column chromatography using silica gel (100–200 mesh) as packing material and 3%

ethyl acetate in hexane as eluent. ^1H NMR (CDCl_3) δ 0.88–1.03 (m, 10H), 1.27–1.52 (m, 24H), 1.62 (m, 4H), 1.81 (m, 8H), 2.53 (m, 4H), 3.24 (t, 4H, $J = 6.6$ Hz), 3.61 (t, 4H, $J = 7.2$ Hz), 3.83 (m, 4H), 3.94 (m, 2H), 4.08 (d, 2H, $J = 13.0$ Hz), 6.69 (t, 2H, $J = 7.4$ Hz), 6.82 (t, 2H, $J = 7.4$ Hz), 6.96 (d, 4H, $J = 7.6$ Hz), 7.05 (d, 4H, $J = 7.6$ Hz). IR: 2561 cm^{-1} (SH). ES-MS: m/z 925.71 (calculated for $4\text{-H}^+ + 2\text{Na}^+$, 926.33); 957.46 (calculated for $4\text{-H}^+ + 2\text{Na}^+ + \text{MeOH}$, 958.37); 996.50 (calculated for $4\text{-H}^+ + 2\text{Na}^+ + \text{K}^+ + \text{MeOH}$, 996.46). Anal. calcd. for $\text{C}_{56}\text{H}_{80}\text{O}_4\text{S}_2$: C, 76.33; H, 9.14; S, 7.20; Found: C, 75.52; H, 9.02; S, 7.05.

2.4 Functionalization of gold nanoparticle with **4** (CFAuNPs, **5**)

All the glass ware used in this reaction were thoroughly cleaned with aquaregia and rinsed with milliQ water and dried. $\text{HAuCl}_4 \cdot 3\text{H}_2\text{O}$ (7.75 mg) was dissolved in milliQ water (0.6 mL) and added 10 mL solution of 40 mM tetra octyl ammonium bromide (TOAB, 0.215 g) in toluene. This biphasic mixture was stirred for 30 min in a 50 mL Erlenmeyer flask and then the aqueous phase was discarded to yield gold (III) TOAB solution. Subsequently, compound **4** was added to the gold (III) TOAB solution with vigorous stirring. After 30 min of stirring, freshly prepared aqueous solution of 0.4M NaBH_4 (7.44 mg in 0.5 mL) was added drop-wise at a rate of approximately 20 μL per 15 s under vigorous stirring. The initial orange colour of gold (III) solution became colourless and then turned to dark brown, the stirring was continued for 3 h after complete addition of NaBH_4 solution. The organic layer was then separated, diluted with methanol (100 mL) and kept in refrigerator for overnight. The precipitate thus obtained was separated by removing the solvent carefully and was purified further by dispersion in toluene (5 mL) followed by addition of methanol (10 mL) and by centrifuge for 10 min at 10,000 rpm speed. This process was repeated twice to remove any unbound compound **4** from CFAuNPs. The residue obtained after centrifuge was again dispersed in toluene (5 mL) and preserved as stock solution of CFAuNPs. This stock solution was used for further experiments. For characterization, IR and UV-Vis spectra, and TEM images were recorded and EDX analysis was carried out.

2.5 Interaction of various metal ions with the CFAuNPs

The stock solution in toluene was diluted by five times with THF and the concentration of the CFAuNPs in

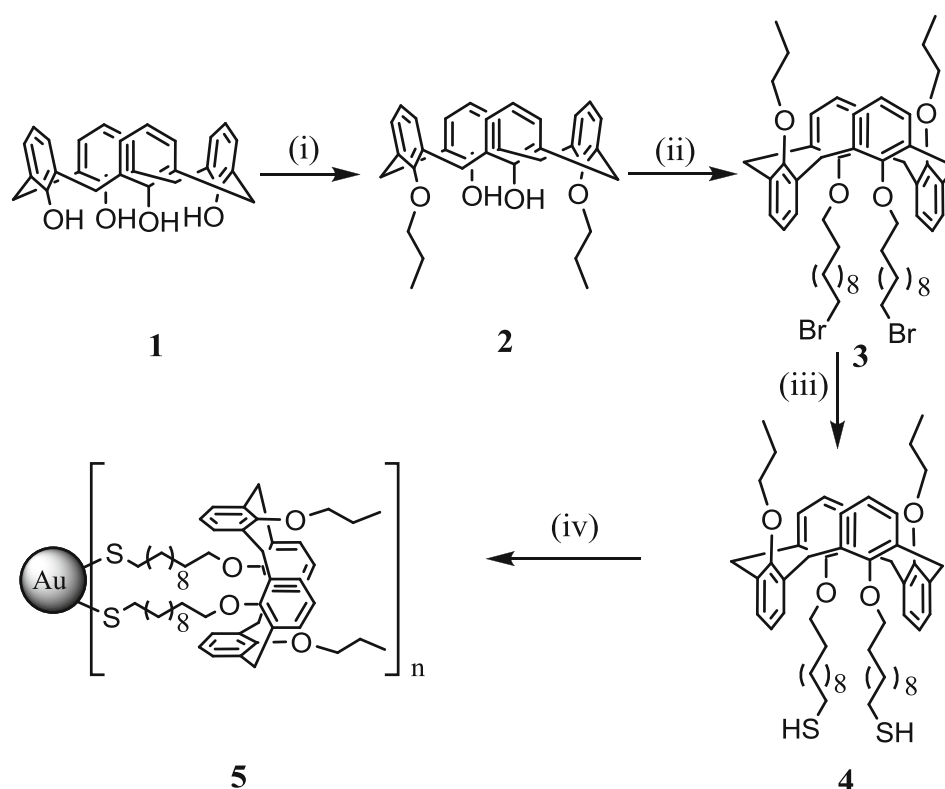
solution was determined from the absorption at 523 nm (λ_{max}) following the literature procedure.⁵² The concentration of the diluted solution was found to be 4.5×10^{-8} M (45 nM), which was used to study ion-binding property with the perchlorate salts of the metal ions Li^+ , Na^+ , K^+ , Ba^{2+} , Mg^{2+} , Fe^{3+} , Cs^+ , Hg^{2+} , Ca^{2+} , Zn^{2+} , Cd^{2+} , Ni^{2+} , Sr^{2+} , Cu^{2+} , Pb^{2+} . The solution (2 mL) of each metal ion (100 μM) was added into the 2 mL solution of the CFAuNPs in a 5 mL volumetric flask and the UV-Vis spectra of the resulting solutions were recorded. For Cu^{2+} ion, a new band around 650 nm was developed and the intensity of the 523 nm band significantly reduced with a red shift to 530 nm. In the case of Pb^{2+} , the 523 nm band was shifted to 544 nm with decrease in intensity and sharp colour change from dark brown to blue.

2.6 UV-Vis spectral changes for CFAuNPs with increasing amount of metal ions

The UV-Vis spectral change for Cu^{2+} and Pb^{2+} were recorded upon addition of increasing amount of metal ions while maintaining the concentration of CFAuNPs constant. The concentrations of the metal ions maintained in the solutions for Cu^{2+} were 10, 20, 30, 40, 50, 60, 70, 80 and 100 μM ; and the same for Pb^{2+} were 50, 80, 110, 150, 175, 200, 210 and 220 μM .

3. Results and discussion

The route for the synthesis of CFAuNPs (**5**) is shown in scheme 1 and details of synthesis and characterization data are given in section 2. Characterization of **3** was done on the basis of elemental analysis, ES-MS and ^1H NMR data. The conformation of the calixarene moiety is confirmed from ^1H NMR data, the multiplets correspond to eight protons in the region δ 3.83–4.08 ppm for the $\text{Ar-CH}_2\text{-Ar}$ methylene groups is characteristic for the 1,3-alternate conformation of the calixarene moiety. Compound **4** was characterized on the basis of elemental (C, H and N) analysis, ES-MS, IR and ^1H NMR data. The elemental analysis and mass data are in excellent agreement with the composition of the compound. The IR spectrum exhibited a band at 2561 cm^{-1} , which is assigned to the SH group. In the ^1H NMR spectrum, the $\text{Ar-CH}_2\text{-Ar}$ methylene protons appeared as multiplets at δ 3.83–4.10 ppm, which confirmed 1,3-alternate conformation of the calixarene unit, as observed for **3**. The methylene protons of the undecane chain appeared in the aliphatic region as multiplets with methylene protons (CH_2) adjacent to SH at δ 2.53 ppm, the signal for other protons appeared in the expected region



Scheme 1. Route for synthesis of functionalized gold nanoparticles. (i) K_2CO_3 , $\text{C}_3\text{H}_7\text{I}$, CH_3CN , reflux 24 h. (ii) K_2CO_3 , 1,11-dibromoundecane, CH_3CN , reflux 48 h. (iii) TBAF, $(\text{Me}_3\text{Si})_2\text{S}$, THF (-5°C). (iv) HAuCl_4 , TOAB, NaBH_4 , toluene.

as reported earlier.^{53,54} The gold nanoparticle was then functionalized by anchoring compound **4** on to the surface of the nanoparticles and the **CFAuNps (5)** was characterized on the basis of IR, UV-vis spectral data, TEM image and EDX analysis. The IR band for SH observed at 2561 cm^{-1} for **4** was not observed in the IR spectra of **5**, which indicated deprotonation of SH for the formation of Au–S bond.^{46,47} The UV-Vis spectra of **5** exhibited absorption band at 523 nm, which is attributed to the surface plasmon resonance (SPR) band of the functionalized gold nanoparticles.^{17,22–29,47} The TEM image of **5** exhibits discrete particles and no aggregation is noted, the average size of the particles determined by TEM is 2–5 nm. The EDX analysis of **5** confirmed the presence of gold (18.26 atomic%) in this material.

3.1 Interaction of CFAuNPs with various metal ions

The interaction of the **CFAuNPs** with various metal ions was monitored by UV-Vis spectral change and also by colour change visualized with naked-eye. The absorption spectra of the **CFAuNPs** was recorded in THF upon addition of the perchlorate salts of various

metal ions ($100\text{ }\mu\text{M}$). Out of the large number of metal ions tested (Li^+ , Na^+ , K^+ , Ba^{2+} , Mg^{2+} , Fe^{3+} , Cs^+ , Hg^{2+} , Ca^{2+} , Zn^{2+} , Cd^{2+} , Ni^{2+} , Sr^{2+} , Cu^{2+} , Pb^{2+}), only Cu^{2+} and Pb^{2+} exhibited significant spectral change (figure S1, see [supplementary information](#)) with sharp colour change from dark brown to green and blue for Cu^{2+} and Pb^{2+} , respectively, detectable by naked-eye (figure 1a and b). The absorption band observed for **CFAuNPs** at 523 nm due to the SPR shifted to 544 nm for Pb^{2+} (figure 1a) and at 650 nm for Cu^{2+} (figure 1b). The intensity of the 523 nm band decreased significantly with the appearance of new bands. The calibration plot of the absorbance at 540 nm against concentration of Pb^{2+} added is given as inset in figure 1a. Similar plot for Cu^{2+} is also shown as inset in figure 1b, where absorbance ratio A_{650}/A_{525} was plotted against concentration of Cu^{2+} ion. It may be noted that as the concentration of the metal ion increases the intensity of the absorbance is linearly enhanced. The detection limit for Cu^{2+} is 0.65 ppm and for Pb^{2+} it is 10.0 ppm. The colour change observed for Pb^{2+} and Cu^{2+} is due to the bathochromic shift of the SPR band and formation of a new SPR band, respectively.

The transmission electron microscopic (TEM) images of **CFAuNPs** were recorded before and after

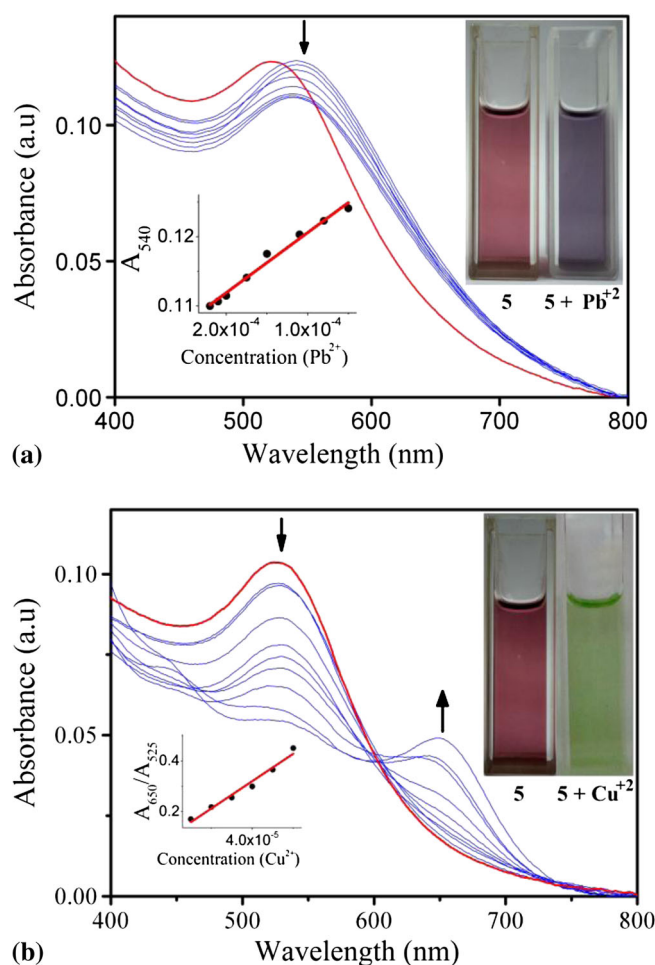


Figure 1. UV-vis spectra depicting gradual decrease of CFAuNPs band at 523 nm and formation of a new band at (a) 544 nm upon addition of Pb^{2+} and (b) 650 nm upon addition of Cu^{2+} . [Inset: their respective colour changes and change of the absorption (a) and the ratio of absorption (b) intensity as a function of concentration of metal ion added.]

the addition of metal ions. The images are presented in figure 2. The average size of the CFAuNPs before the addition of metal ion was 2–5 nm (figure 2a),

which increases to 7–9 nm (figure 2b) upon addition of Cu^{2+} and 13–16 nm after addition of Pb^{2+} ions (figure 2c). The presences of Cu^{2+} and Pb^{2+} in the aggregated nanoparticles were identified using STEM-EDX mapping (figures S2, S3 and S4). The line profiles from the STEM-EDX map are given in figure 3, indicating relative position of gold nanoparticles. It is clearly evident that the average separation between gold nanoparticles in CFAuNPs has decreased from few tens of nanometers to a few nanometers after addition of metal ions due to aggregation.

Similar results have been obtained from dynamic light scattering study (DLS). The size distribution profiles obtained from DLS data, before and after addition of metal ions is given in figure 4. It can be seen in the figure that the hydrodynamic radius (RH) of CFAuNPs (5) is around 35 nm, which increases up to 3.6 μm (in case of Cu^{2+}) and 247 μm (in case of Pb^{2+}), as evident by the most intense peaks in DLS plot, after addition of metal ions. Apart from this prime peak, one less intense peak has also been observed for both the metals, which is due to different type of aggregation with less hydrodynamic radius (RH). As discussed earlier the sizes of CFAuNPs were found to be around 2–5, 7–9 and 13–16 nm by TEM, which may be attributed to the core radius of the nanoparticles. Significant difference in the size of the nanoparticle as measured by DLS and TEM may be attributed to the fact that the DLS measures the hydrodynamic size, whereas TEM measures only the metallic core size.⁵⁵

3.2 Mechanistic aspects of interaction with metal ions

The average sizes of the CFAuNPs obtained from TEM images after addition of metal ions is higher for Pb(II) (13–16 nm) compared to that of Cu(II) (7–9 nm), similar trend is also observed for DLS study, 247 μm for Pb(II) and 3.6 μm for Cu(II). According to this data,

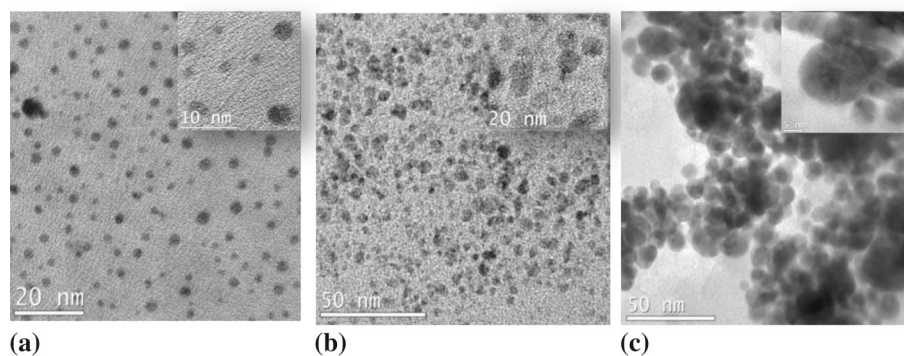


Figure 2. TEM images of CFAuNPs, (a) before and (b) after addition of Cu^{2+} and (c) Pb^{2+} in THF. The overall concentration of CFAuNPs remained same in all the three cases.

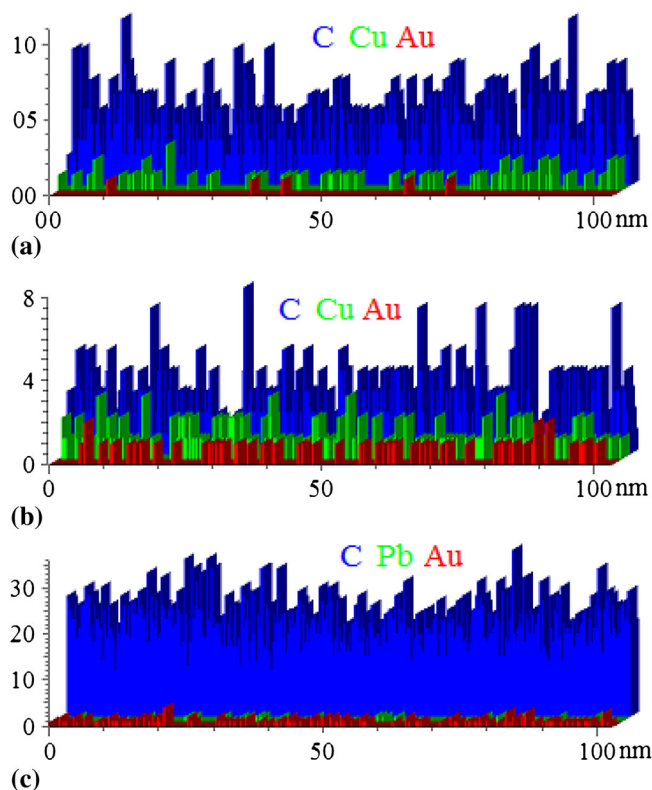


Figure 3. Line scan from the STEM-EDX elemental mapping of (a) CFAuNPs and upon addition of (b) Pb^{2+} and (c) Cu^{2+} .

the λ_{max} value in UV-visible spectra after addition of metal ions should be higher for $\text{Pb}(\text{II})$ compared to that of $\text{Cu}(\text{II})$ but the observation is reverse. It may also be noted that in case of $\text{Pb}(\text{II})$, the λ_{max} of the SPR band of CFAuNPs is shifted from 523 to 544 nm, whereas for $\text{Cu}(\text{II})$ a new second SPR band is appeared at 650 nm

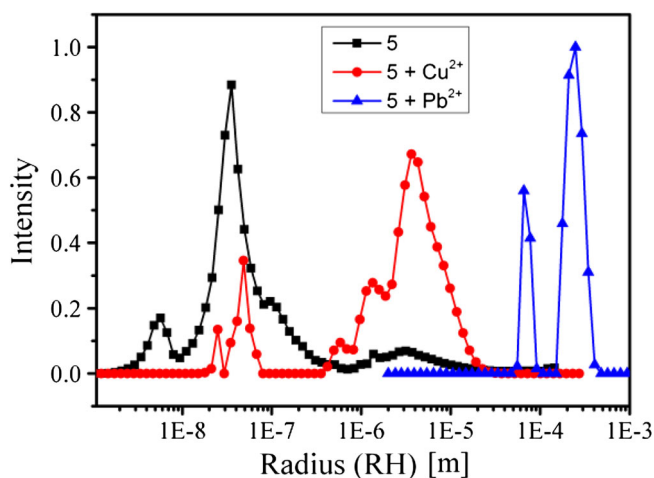


Figure 4. Size distribution curve of CFAuNPs before and after addition of metal ions, indicating enhancement in hydrodynamic radii after addition of metal ion.

with decreasing the intensity of 523 nm band. This is apparently contradictory observation suggesting that the mechanism involved in the process is different for the two metal ions. The bathochromic shifts observed for $\text{Pb}(\text{II})$ is probably associated with the aggregation of nanoparticles according to MIE theory.⁵⁶ The aggregation of the CFAuNPs is due to the interaction of metal ion with the calixarene moiety. The calix[4]arene moiety is in 1,3-alternate conformation, therefore the propyl substituted oxygen donor atoms at the upper rim of the calix moiety and the delocalization of the π electrons of the aromatic rings can create an electron-rich donor centre and two or more such units can create a cavity, in which the positively charged metal ion can encapsulate as shown in figure 5 resulting in metal-induced aggregation of the nanoparticles.^{57,58} The colour and spectral change observed for $\text{Pb}(\text{II})$, is therefore due to the inter particle plasmon coupling because of the metal ion (Pb^{2+}) induced aggregation of the CFAuNPs.^{22,32,33,40,43,59,60} For $\text{Cu}(\text{II})$, since it reduces easily, it has been reported that in contact with gold nanoparticles the metal ion can get reduced forming a core-shell or an AuCu alloy.⁶¹ This phenomenon has been termed as ‘anti-galvanic exchange’ and it changes the average size of the gold nanoparticles and also inter-particle distance causing colour change of the solution with the growing of a new SPR band. To check this hypothesis, two experiments with the aid of powder XRD and UV-vis absorption study were carried out. For powder XRD experiments, the CFAuNPs were separated by centrifuge before and after addition of metal ions and for the mass with metal ions, the solids were washed three times using THF to remove free metal ion, if any. The solids were then taken on a plate and powder XRD of the samples was recorded. The powder diffraction pattern for CFAuNPs and that after addition of $\text{Pb}(\text{II})$ are shown in figures S5 and S6 (supplementary information); and the diffractogram after interaction with $\text{Cu}(\text{II})$ is shown in figure 6. In the diffractogram of CFAuNPs (figure S5), the peaks for Cu are identified (JCPDS No. 01-071-4615), there are some additional peaks, which have not been well resolved due to poor

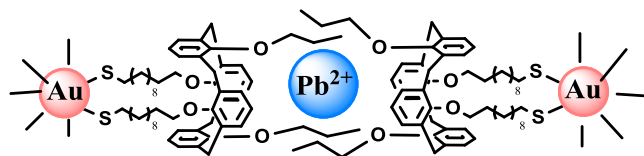


Figure 5. Proposed mechanism of the $\text{Pb}(\text{II})$ induced aggregation of the calixarene functionalized gold nanoparticles.

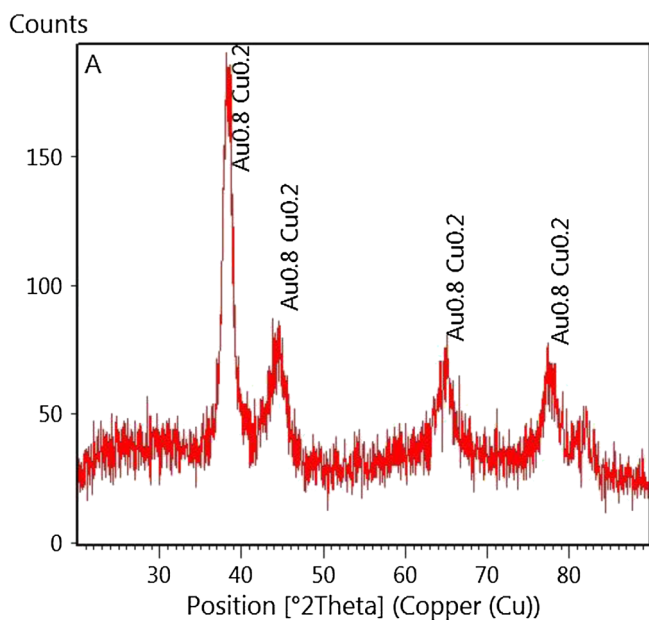


Figure 6. Powder X-Ray diffraction pattern of CFAuNPs after interaction with $\text{Cu}(\text{ClO}_4)_2$, the solid mass was isolated by centrifuge (diffractogram matched with the JCPDS No. 01-072-5241).

quality of the diffractogram and they may be due to calixarene moiety. The diffractogram shown in figure 6 matched well with the JCPDS No. 01-072-5241, which corresponds to AuCu alloy and no other separate prominent peak for Au or Cu(II) is noted. For Pb(II), there are large number of peaks and most of them are accounted with the JCPDS Nos. 98-003-6296 (Pb_3O_4), 04-006-6727 (Pb) and 04-003-7288 (Au), which suggest the metal ions (Au and Pb) exist in separate identity (figure S6). The unaccounted peaks might be due to calixarene moiety. This observation, therefore suggest the ‘anti-galvanic exchange’ and ‘metal-induced aggregation’ mechanisms for Cu(II) and Pb(II), respectively. For Cu(II), the reversibility of the binding/encapsulation of metal ion is also checked by UV-vis experiment with the aid of dithioamide, which is known for strong binding with Cu(II) and uses for gravimetric analysis of Cu(II).⁶² The UV-vis spectrum of CFAuNPs, that after addition of Cu(II) with λ_{max} of the SPR band at 650 nm and the spectrum upon addition of the dithioamide ligand into the above solution containing Cu(II) are shown in figure 7. It may be noted that dithioamide being a very strong ligand for Cu(II) compared to calixarene, the new SPR band at 650 nm grown after addition of Cu(II) neither shifted nor disappeared and also there is no indication to regenerate the original 523 nm band due to CFAuNPs. This experiment also supports the formation of AuCu alloy by ‘anti-galvanic exchange’ process.

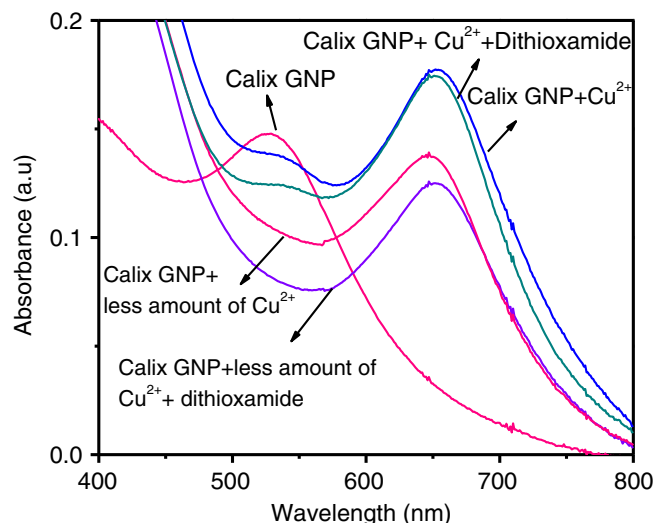


Figure 7. UV-vis spectra of CFAuNPs, recorded before and after addition of Cu^{2+} with two different concentrations. The spectral changes after addition of dithioamide into the Cu^{2+} containing solution are also shown.

4. Conclusions

In summary, we prepared calixarene functionalized gold nanoparticles as colorimetric sensor for metal ions. Out of a large number of metal ions, it exhibits distinct colour changes in presence of Cu^{2+} and Pb^{2+} with high sensitivity, detectable with naked eye. The colour change for Pb(II) is due to the red shift of the plasmon band, which attributed to the inter particle plasmon coupling because of the metal-induced aggregation of the CFAuNPs. For Cu(II), the colour change is due to growing of a new SPR band because of the formation of AuCu alloy due to anti-galvanic reduction of Cu(II). The aggregation is confirmed by TEM and the presence of Cu^{2+} and Pb^{2+} is confirmed by elemental mapping and EDX analysis. This is a rare example of colourimetric sensor for metal ions with calixarene functionalized gold nano particles.

Supplementary information

The electronic supporting information, STEM-EDX mapping of the aggregated CFAuNPs upon addition of metal ions (figures S1–S6) are available in www.ias.ac.in/chemsci.

Acknowledgements

We thank the Department of Science and Technology (DST), Government of India, for financial support. We thank reviewers and editor for very

useful suggestions, which helped to elucidate mechanistic aspect of the interaction with metal ions. We thank the Council of Scientific and Industrial Research (CSIR), New Delhi for generous support towards infrastructures and core competency development. RG and DM gratefully acknowledge the CSIR for awarding Senior Research Fellowship (SRF). We thank Dr S Patra, Dr V P Boricha, A K Das and V Agrawal for useful discussion and for recording NMR, TEM, mass, and IR spectra, respectively.

References

- De Silva A P, Gunaratne H Q N, Gunnlaugsson T, Huxley A J M, McCoy C P, Rademacher J T and Rice T E 1997 *Chem. Rev.* **1515**
- Valeur B and Leray I 2000 *Coord. Chem. Rev.* **205** 3
- Beer P D and Hayes E J 2003 *Coord. Chem. Rev.* **240** 167
- Yoon J, Kim S K, Sing N J and Kim K S 2006 *Chem. Soc. Rev.* **35** 355
- Kim J S and Quang D T 2007 *Chem. Rev.* **107** 3780.
- Environmental Protection Agency U S 1989 *US EPA 625/4-89/024* Office of Water, Washington DC 20460
- Hamilton J W, Kaltreider R C, Bajenova O V, Inhat M A, McCaffrey J, Turpie B W, Rowell E E, Oh J, Nemeth M J, Pesce C A, Lariviere J P and Environ J 1998 *Health* **106** 1005
- Aragay G, Pons J and Merkoci A 2011 *Chem. Rev.* **111** 3433
- Fabbri L and Pooggi A 1995 *Chem. Soc. Rev.* **24** 197
- Uauy R, Olivares M and Gonzalez M 1998 *Am. J. Clin. Nutr.* **67** 952S
- Waggoner D J, Bartnikas T B and Gitlin J D 1999 *Neurobiol. Dis* **6** 221
- Tapia L, Suazo M, Hodar C, Cambiazo V and Gonzalez M 2003 *Bio. Metals* **16** 169
- Schroeder H A and Tipton I H 1968 *Environ. Health* **17** 965
- Bridgewater B M and Parkin G 2000 *J. Am. Chem. Soc.* **122** 7140
- Lewis J A and Cohen S M 2004 *Inorg. Chem.* **43** 6534
- Yoosaf K, Ipe B I, Suresh C H and Thomas K G 2007 *J. Phys. Chem. C* **111** 12839
- Yan H, Luo J, Xie H M, Xie D X, Su Q, Yin J, Wanjala B N, Diao H, An D L and Zhong C J 2011 *Phys. Chem. Chem. Phys.* **13** 5824
- Kim J S and Quang D T 2007 *Chem. Rev.* **107** 3780
- Patra S and Paul P 2009 *Dalton Trans.* 8683
- Ipe B I, Yoosaf K and Thomas K G 2006 *J. Am. Chem. Soc.* **128** 1907
- Muthukumar C, Kesarkar S D and Srivastava D N 2007 *J. Electroanal. Chem.* **602** 172
- Kim Y J, Johnson R C and Hupp J T 2001 *Nano Lett.* **1** 165
- Arduini A, Demuru D, Pochini A and Secchi A 2005 *Chem. Commun.* 645
- Beer P D, Cormode D P and Davis J J 2004 *Chem. Commun.* 414
- Yang W, Gooding J J, He Z, Li Q and Chen G 2007 *J. Nanosci. Nanotechnol.* **7** 712
- Chen P and He C 2004 *J. Am. Chem. Soc.* **126** 728
- Liu J and Lu Y 2007 *Chem. Comm.* 4872
- Talapin D V, Lee J S, Kovalenko M V and Shevchenko E V 2010 *Chem. Rev.* **110** 389
- Lin Y W, Huang C C and Chang H T 2011 *Analyst* **136** 863
- Luo M, Oliver G K and Frechette J 2012 *Soft Matter* **8** 11923
- Jin R, Wu G, Li Z, Mirki C A and Schatz G 2003 *J. Am. Chem. Soc.* **125** 1643
- Liu D, Chen W, Sun K, Deng K, Zhang W, Wang Z and Jiang X 2011 *Angew. Chem. Int. Ed.* **123** 4103
- Kim Y R, Mahjan R K, Kim J S and Kim H 2010 *Appl. Mater. Interfaces* **2** 292
- Wang H, Wang Y, Ji J and Yan R 2008 *Anal. Chem.* **80** 9021
- Sato K, Hosokawa K and Maeda M 2007 *Anal. Sci.* **23** 17
- Kado S, Furui A, Akiyama Y, Nakahara Y and Kimura K 2009 *Anal. Sci.* **25** 261
- Uehara N 2010 *Anal. Sci.* **26** 1219
- Sudarsan T, Srinivas H and Prasad B L V 2007 *J. Nanosci. Nanotechnol.* **7** 2683
- Ray P C 2010 *Chem. Rev.* **110** 5332
- Liu C W, Hsieh Y T, Huang C C, Lin Z H and Chang H T 2008 *Chem. Commun.* 2242
- Lee J S, Han M S and Mirkin C A 2007 *Angew. Chem. Int. Ed.* **46** 4093
- Savage A C and Pikramenou Z 2011 *Chem. Commun.* 6431
- Slocik J M, Zabinski Jr J S, Philips D M and Naik R R 2008 *Small* **4** 548
- You C C, Agasti S S and Rotello V M 2008 *Chem. Euro. J.* **14** 143
- Patel G, Kumar A, Pal U and Menon S 2009 *Chem. Commun.* 1849
- Lin S Y, Liu S Y, Lin C M and Chen C H 2002 *Anal. Chem.* **74** 330
- Patel G and Menon S 2009 *Chem. Commun.* 3563
- Tshikudo T R, Demuru D, Wang Z, Brust M, Secchi A, Arduini A and Pochini A 2005 *Angew. Chem. Int. Ed.* **44** 2913
- Gutsche D C, Levine J A and Sujeeth P K 1985 *J. Org. Chem.* **50** 5802
- Casnati A, Pochini A, Ungaro R, Ugozzoli F, Arnauad F, Fanni S, Schwing M J, Egberink R J M, de Jong F and Reinhoudt D N 1995 *J. Am. Chem. Soc.* **117** 2767
- Hu J and Fox M A 1999 *J. Org. Chem.* **64** 4959
- Liu X, Atwater M, Wang J and Huo Q 2007 *Colloids & Surfaces* **58** 3
- Snow A W, Foos E E, Coble M M, Jernigan G G and Ancona M G 2009 *Analyst* **134** 1790
- Arduini A, Demuru D, Pochini A and Secchi A 2005 *Chem. Commun.* 645
- Kasture M B, Patel P, Prabhune A A, Ramana C V, Kulakarni A A and Prasad B L V 2008 *J. Chem. Sci.* **120** 515
- Si S, Raula M, Paira T K and Mandal T K 2008 *Chem. Phys. Chem.* **9** 1578

57. Hussain I, Brust M, Barauskas J and Cooper A I 2009 *Langmuir* **25** 1934
58. Link S and Sayed M E 2009 *Int. Rev. Phys. Chem.* **19** 409
59. Huang C C and Chang H T 2007 *Chem. Commun.* 1215
60. Toma H E, Zamarion V M, Toma S H and Araki K 2010 *J. Braz. Chem. Soc.* **21** 1
61. Wu Z 2012 *Angew. Chem. Int. Ed.* **51** 2934
62. Furman N H 1962 *Standard methods of chemical analysis*, 6th Ed. 396, Princeton NJ, Van Nostrand Company Inc.